Available online at www.sciencedirect.com
ScienceDirect
International Journal of Heat and Mass Transfer 51 (2008) 1130–1138
International Journal of HEAT and MASS TRANSFER
www.elsevier.com/locate/ijhmt

Experiments on heat transfer enhancement from a heated square cylinder in a pulsating channel flow

Tae Ho Ji [a], Seo Young Kim [b,*], Jae Min Hyun [a]

[a] Department of Mechanical Engineering, Korea Advanced Institute of Science and Technology, Daejon 305-701, Republic of Korea
[b] Thermal/Flow Control Research Center, Korea Institute of Science and Technology, Seoul 130-650, Republic of Korea

Received 22 December 2006; received in revised form 24 April 2007
Available online 22 October 2007

Abstract

Experiments have been performed to investigate heat transfer enhancement from a heated square cylinder in a channel by pulsating flow. For all the experiments, the amplitude of the pulsating flow is fixed at $A = 0.05$. The effects of the Reynolds number based on the mean flow velocity ($Re = 350$ and 540), the pulsating frequency (0 Hz $< f_p <$ 60 Hz) and the blockage ratio of the square cylinder ($\beta = 1/10$, 1/8, and 1/6) on convective heat transfer are examined. The measured Strouhal numbers of shedding vortices for non-pulsating ($A = 0$) steady inlet flow are compared with the previously published data, and good agreement is found. The "lock-on" phenomenon is clearly observed for a square cylinder in the present flow pulsation. When the pulsating frequency is within the lock-on regime, heat transfer from the square cylinder is substantially enhanced. In addition, the influence of the Reynolds number and the blockage ratio on the lock-on occurrence is discussed in detail.

Keywords: Lock-on; Pulsating flow; Heat transfer enhancement; Square cylinder

1. Introduction

Flow over a bluff body has been of practical importance in many engineering applications. Most researches have focused on the flow over circular cylinders. Excellent reviews on this configuration were given by Zdravkovich [1] and Williamson [2]. For the flow over a square cylinder, the separation mechanism and the dependence of the shedding frequency on the Reynolds number are the major issues. For a flow over a square cylinder, the separation points are fixed at its leading or trailing edges. It is generally believed that the aerodynamic coefficients are less dependent on the Reynolds number for a square cylinder. In contrast to the large number of publications on the flow past circular cylinders, the study on square cylinders has not been numerous. Furthermore, most investigations were concerned with the flow characteristics without heat transfers [3–8].

Several papers described the convective heat transfer characteristics from square cylinders. Kelkar and Patankar [9] discussed the overall heat transfer from a square cylinder in unsteady flow. Laminar channel flows with a square cylinder were studied numerically and experimentally by Suzuki and Suzuki [10]. They observed that induced vortex near the heat transfer surface entrains cooler fluid from the downstream region, and a this fluid motion contributes to enhancement of heat transfer. Shuja et al. [11] showed that a vortex attached to the body enhanced heat transfer while a detached vortex lowered heat transfer.

For the flow past a stationary cylinder, it is known that vortices are shed with a constant natural frequency, St, at a particular Reynolds number. Within a narrow range of externally forced frequency, vortex shedding can be controlled by the oscillation of the cylinder (or flow pulsation). In this case, remarkable increases in the lift and drag forces are observed. This is referred to as "lock-on," or "wake

* Corresponding author. Tel.: +82 2 958 5683; fax: +82 2 568 5689.
E-mail address: seoykim@kist.re.kr (S.Y. Kim).

0017-9310/$ - see front matter © 2007 Published by Elsevier Ltd.
doi:10.1016/j.ijheatmasstransfer.2007.04.015

Nomenclature

A	pulsating amplitude or cylinder displacement
B	side length of a square cylinder (mm)
E	heat transfer enhancement factor, Nu_p/Nu_s
f	dimensional frequency (Hz)
f_p	pulsating frequency (Hz)
f_s	shedding frequency (Hz)
f_{so}	natural shedding frequency (Hz)
h	convective heat transfer coefficient (W/m^2 K)
H	height of flow channel (mm)
k	thermal conductivity of air (W/m K)
L	length of flow channel (mm)
Nu	Nusselt number
q	input heat flux (W/m^2)
q_{loss}	heat loss (W/m^2)
Re	Reynolds number, U_0B/v
St	Strouhal number, fB/U_0
T	local surface temperature (K)
T_i	inlet air temperature (K)
U_i	inlet air velocity (m/s)
U_0	time-averaged inlet air velocity (m/s)
W	channel width (mm)
X	streamwise coordinate (mm)
X_d	distance from the channel outlet to downstream face of the cylinder (mm)
X_u	distance from the channel inlet to upstream face of the cylinder (mm)
Y	transverse coordinate (mm)

Greek symbols

β	blockage ratio, B/H
v	kinematic viscosity (m^2/s)
ω	angular frequency (rad/s)

Subscripts

p	pulsating component
s	steady-state component

capture" or "vortex resonance" phenomenon. For transverse oscillations, the lock-on occurs when the forced oscillating frequency approaches the natural shedding frequency resulting in a considerable increase in the drag force with the vortices being shed at the same frequency as the oscillation frequency. For in-line oscillations or in-line flow pulsation, the lock-on is observed at the oscillation frequency which is twice the natural shedding frequency. This implies that the vortex shedding occurs at half the oscillation frequency [12–18]. The lock-on phenomenon is observed in many practical engineering applications, i.e, the offshore exploration, the marine hydrodynamics, and the power generation. Recently, this phenomenon can be used to intensify the wake flow to enhance heat transfer, mixing and combustion in the electronics devices, lab on a chip, fuel cell and so on.

Previous studies have delineated the effects of lock-on phenomenon on the flow fields. The influence of the lock-on phenomenon on mass and heat transfers has not been studied in detail. Prior numerical and experimental endeavors have shown that the flow pulsation over a circular cylinder leads to increased heat and mass transfers when the lock-on phenomenon takes place [12,19–21].

The present study aims to examine experimentally the influence of flow pulsation on the convective heat transfer from a heated square cylinder in a channel, as shown in Fig. 1. The mean-flow Reynolds number, the flow pulsation frequency, and the blockage ratio of the square cylinder are the principal parameters. Based on the experimentally obtained data, the lock-on phenomenon for a square cylinder in a pulsating channel flow will be depicted. In particular, it will be of interest to analyze the effect of lock-on on the overall heat transfer from a square cylinder.

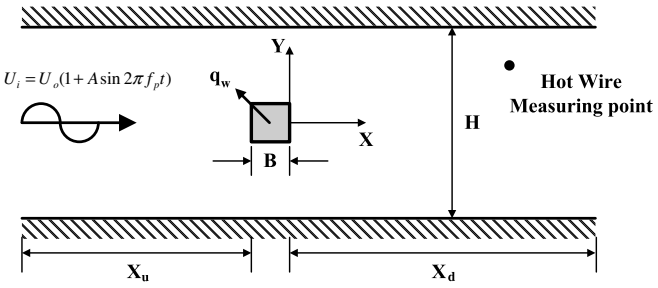

Fig. 1. Schema of a heated square cylinder in a channel.

2. Experimental apparatus and procedure

A schematic diagram of the present experimental apparatus is shown in Fig. 2. The experiments were conducted in a channel fabricated with 10 mm thick Plexiglas of width $W = 150$ mm and length $L = 960$ mm. The height H was varied in the range of 90–150 mm. This gives the blockage ratio (β) from 1/6 to 1/10. A steady main airflow was supplied by a DC fan (Sanyo Denki, 109E1724H543). A preheater was installed behind the DC fan to keep the inlet air temperature constant during the experimental runs. Three-stage mesh screens and a honeycomb were installed to produce a uniform inlet flow with low turbulence intensity. The uniformity of inlet airflow was confirmed by measuring the velocity distribution with a hot-wire anemometer (Dantec StreamLine® System) (see Fig. 3). A DC power supply (Agilent, E3634A) was connected to the DC fan, which adjusted the airflow rate in the test section. The inlet air velocity U_i tested ranged from 0.37 m/s to 0.57 m/s, and the turbulence intensity at the inlet was less than 0.8%. The side length of a square cylinder (B), made of aluminum, was 15 mm. A square cylinder was installed at $X_u = 60$ mm and $X_d = 275$ mm in the channel as shown in Fig. 1.

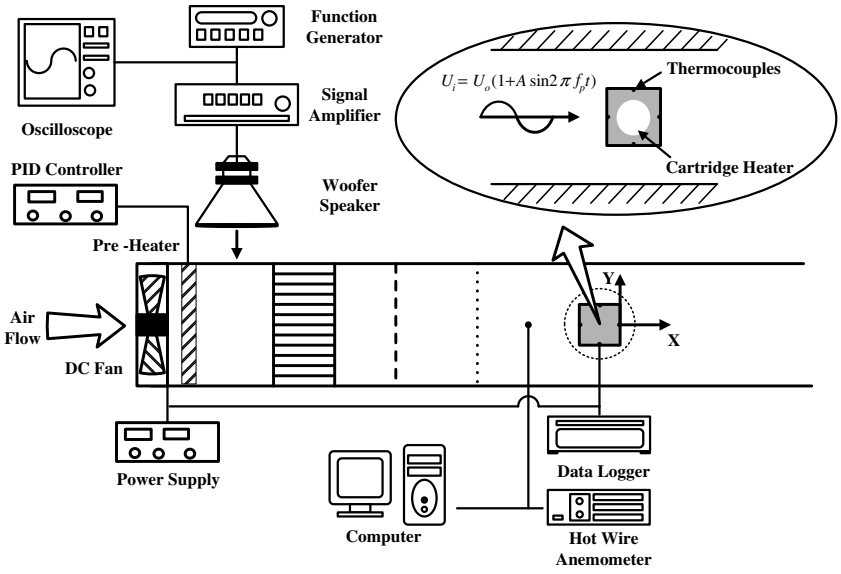

Fig. 2. Experimental apparatus.

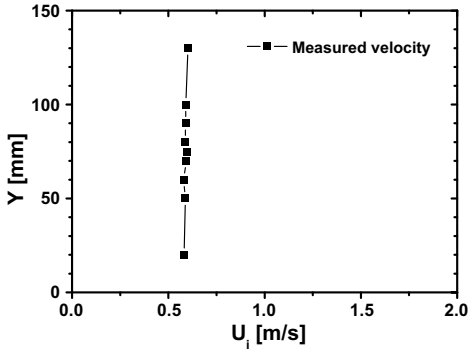

Fig. 3. The measured inlet velocity, U_i, according to the channel height at $Re = 540$, $\beta = 1/10$.

A 300 mm diameter woofer speaker, mounted on a cubic chamber, was used to produce an oscillatory flow. The cubic chamber for the woofer speaker was connected to an air-mixing plenum upstream of the channel with a flexible tube. The flexible tube was employed to reduce mechanical vibration. A function generator (HP, 33120A) provided a sinusoidal signal with a setting frequency, and the signal was amplified by a signal amplifier (Inkel, AX7030G). The amplified signal was sent to the woofer speaker via a digital oscilloscope (LeCroy, 9310A) to confirm the input frequency and voltage.

To generate uniform heat from the square cylinder, a cylindrical cartridge heater was embedded into the square cylinder using thermal compound (Electrolube, TCR75S). The cartridge heater was controlled by a DC power supply (Agilent, E3634A). For all the experimental runs, the power input was kept at 3 W.

Temperatures were measured by T-type thermocouples (Omega AWG36). The air temperature at the inlet and the wall surface temperature of the square cylinder were measured. Four thermocouples to measure the surface temperature were groove-installed on the surfaces of the square cylinder using thermal compound (Electrolube, TCR75S), as shown in Fig. 2. The temperature at the surface was estimated by analyzing one-dimensional conduction from the groove. The wall surface temperature was determined by the arithmetic mean of estimated temperatures.

The experiment was started by heating up the heater and supplying air into the channel with no flow pulsation. The thermally steady state was declared when the variation of measured temperatures was less than ± 0.1 °C for 10 min. After reaching the steady state, all the temperature data were recorded by a data logger (Yokogawa, DS 400). After the steady state temperature data were collected, the pulsating flow was imposed by the acoustic woofer.

Figs. 3 and 4 illustrate sample velocity signals and their power spectra. The time-varying flow velocity was measured at 60 mm upstream of the square cylinder. A hot-wire anemometer was used to determine the pulsating velocity amplitude and the mean-flow Reynolds number. These results indicate that the acoustic woofer produces high-quality flow pulsation in the channel. In the present experiments, the pulsation frequency was varied in the range of 0–60 Hz, and the velocity amplitude of pulsation (A) was fixed at 0.05. To measure the vortex shedding frequency generated from the square cylinder, a hot-wire probe was installed at $X = 6B$ and $Y = 2B$. The measured time signal of the fluctuating velocity was post-processed using the Fast Fourier Transform to acquire the vortex shedding frequency. After reaching the time-periodic steady state, the temperature data were stored in the data acquisition system.

3. Data reduction

The mean-flow Reynolds number Re and the Strouhal number St are defined as

$$Re = \frac{U_0 B}{\nu}, \tag{1}$$

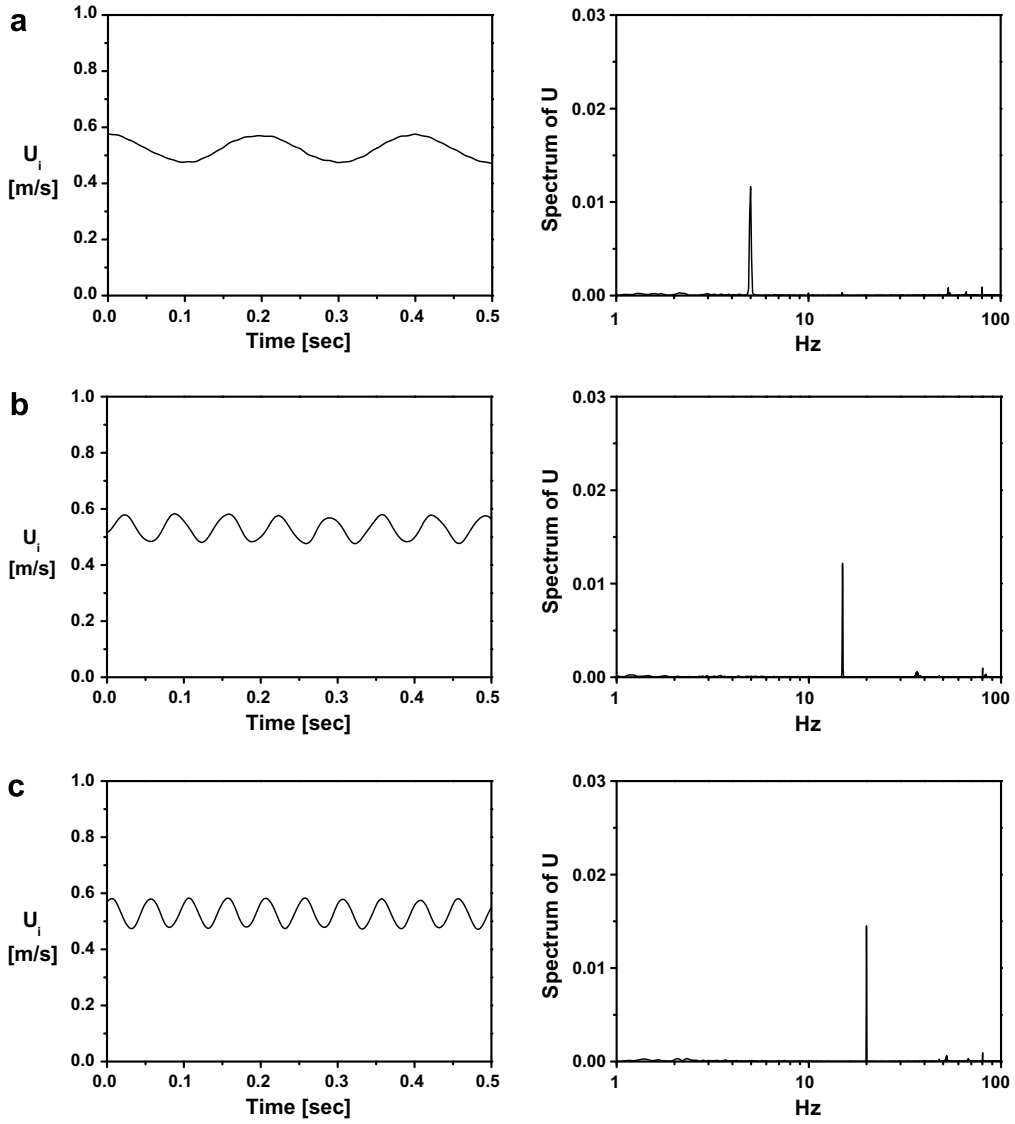

Fig. 4. Exemplary plots of the measured velocity, U_i and its power spectrum at $Re = 540$, $\beta = 1/10$. (a) $f_p = 5$ Hz; (b) $f_p = 15$ Hz; (c) $f_p = 20$ Hz.

$$St = \frac{fB}{U_0}, \tag{2}$$

where U_0, B, and f are the time-averaged inlet flow velocity, the side length of square cylinder, and the frequency, respectively. The Nusselt number Nu is expressed in terms of the actual heat input and the surface temperature. Thus,

$$Nu = \frac{hB}{k} = \frac{q_w B/k}{(T_w - T_i)}, \tag{3}$$

$$q_w = q - q_{loss}. \tag{4}$$

Here, q is total heat flux supplied by the cartridge heater, and q_{loss} is the heat loss conducted through the block side walls.

The uncertainties in the present experiments were estimated by the single-sample experimental analysis by Kline and McClintock in Ref. [22]. The uncertainty in the Nusselt number, δNu, is estimated as:

$$\frac{\delta Nu}{Nu} = \left[\left(\frac{\delta q_w}{q_w}\right)^2 + \left(\frac{\delta(T_w - T_i)}{(T_w - T_i)}\right)^2 + \left(\frac{\delta B}{B}\right)^2 + \left(\frac{\delta k}{k}\right)^2\right]. \tag{5}$$

In summary, typical uncertainties for the Nusselt number and the Reynolds number were estimated to be 3.4% and 3.5%, at the 95% confidence level, respectively (see Table 1).

Table 1
Experimental uncertainties

Parameters	Values
Velocity	±0.5%
Temperature	±0.1 °C
Conductivity	±0.2%
Kinematic viscosity	±0.25%
Heat input	±1.7%
Nusselt number	±3.4%
Reynolds number	±3.5%

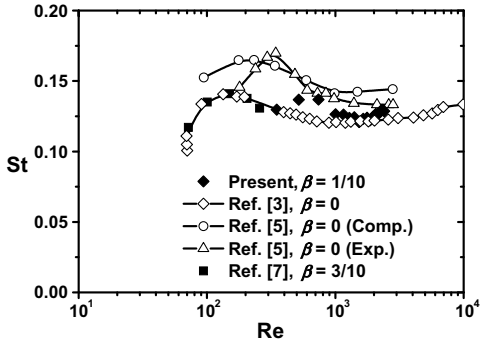

Fig. 5. Comparison of the measured Strouhal numbers *St* with the previous results for a square cylinder.

4. Results and discussion

In an effort to verify the reliability of the present experimental setup and data reduction procedure, some preliminary experiments were carried out for a non-pulsating steady flow ($A = 0.0$) with a square cylinder located in a uniform flow. Fig. 5 shows the Strouhal numbers computed using the natural shedding frequencies of the previously reported results [3,5,7]. Minor discrepancies are attributed to the differences in the main flow turbulence intensity, the blockage ratio [5], the cylinder side wall effect and the sharpness of cylinder edges, among others.

Figs. 6 and 7 demonstrate "the lock-on" phenomenon. When the incoming flow is non-pulsating ($A = 0.0$) as shown in Fig. 6a, the vortex shedding pattern in the wake is characterized by the natural shedding frequency,

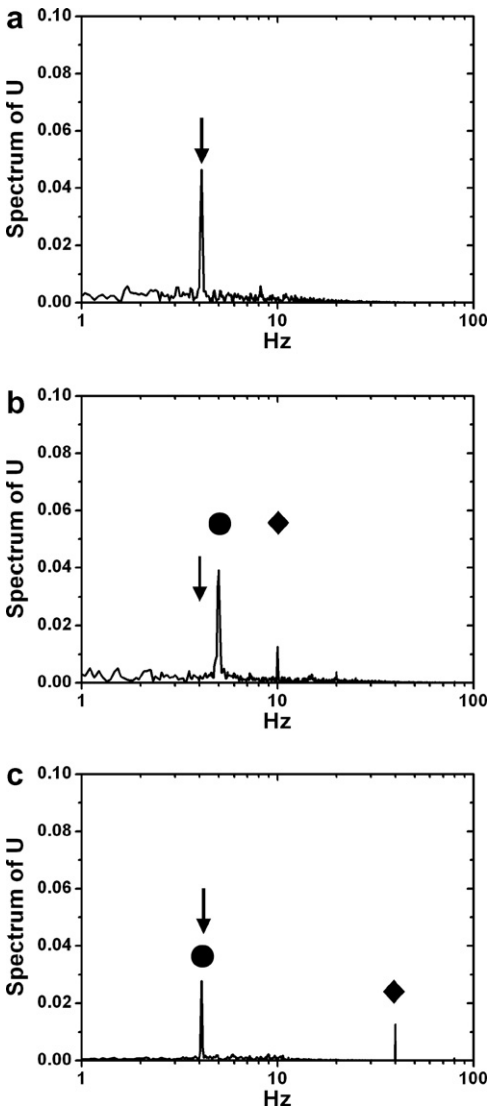

Fig. 6. Power spectra of the measured velocity in wake at $Re = 540$, $\beta = 1/10$ ($f_{so} = 4.1$ Hz): ♦, pulsating frequency (f_p); ●, shedding frequency (f_s). (a) $f_p = 0$ Hz; (b) $f_p = 10$ Hz; (c) $f_p = 40$ Hz (an arrow indicate the natural shedding frequency f_{so}).

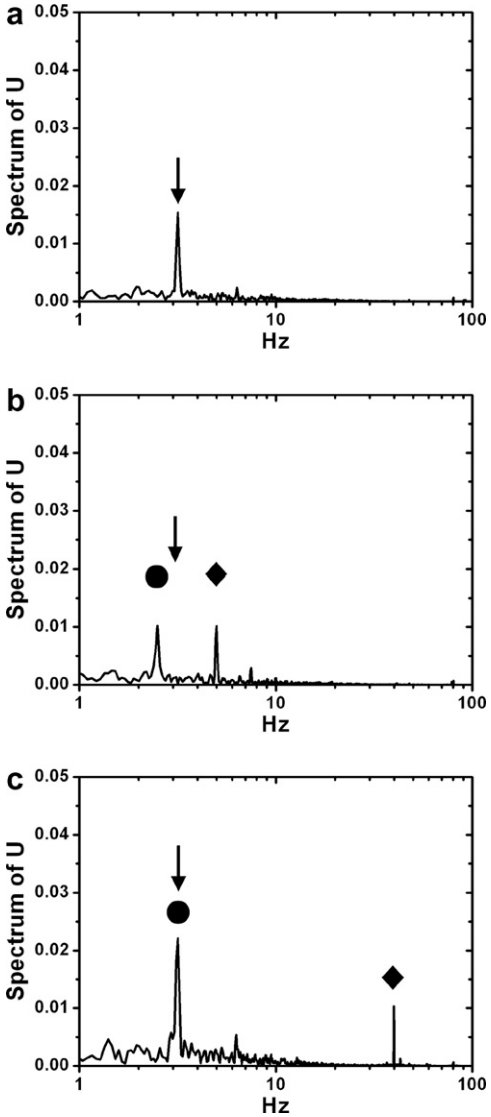

Fig. 7. Power spectra of the measured velocity in wake at $Re = 350$, $\beta = 1/10$ ($f_{so} = 3.2$ Hz): ♦, pulsating frequency (f_p); ●, shedding frequency (f_s). (a) $f_p = 0$ Hz; (b) $f_p = 5$ Hz; (c) $f_p = 40$ Hz (an arrow indicate the natural shedding frequency f_{so}).

$f_{so} \approx 4$ Hz. When f_p is far away from f_{so} (see Fig. 6c), one peak is clearly seen at the natural shedding frequency f_{so} (the arrow indicates the natural shedding frequency for the non-pulsating flow). The vortex shedding frequency marked by the solid circle is identical to the natural shedding frequency. Another peak at the external pulsating frequency of $f_p = 40$ Hz is noted for the wake flow. As f_p approaches twice the natural shedding frequency f_{so}, however, the "lock-on" phenomenon is evident, as seen in Fig. 6b. The vortex shedding in the wake is characterized by the frequency $f_s \approx 5$ Hz, which is $\frac{1}{2} f_p$. The original vortex shedding frequency of $f_{so} \approx 4$ Hz (marked by the arrow) disappears. These features of lock-on have been reported for unsteady fluid dynamics for circular cylinders [12–18]. A similar trend is found in Fig. 7 for a smaller Reynolds number.

The iso-lines of turbulence intensity ($\equiv U_{rms}/U_0$) for various pulsating frequencies f_p are exhibited in Fig. 8. When the pulsating component is added to the incoming flow, the iso-lines reveal a substantial change of the turbulence intensity in the near-wake of the cylinder. The turbulence intensity increases, and a high turbulence intensity zone appears in the central part of the wake when the lock-on occurs, i.e., $f_p = 6$–10 Hz (see 8b and c). This is due to the shrinking of vortex size at the lock-on. A similar phenomenon has been reported in the previous studies for circular cylinders [12–15].

Fig. 9 shows the relationship between the vortex shedding frequency f_s and the pulsation frequency f_p for various blockage ratios ($\beta = 1/10$, 1/8 and 1/6) at $Re = 540$. When f_p/f_{so} is less than 1.5, f_s is slightly reduced from f_{so}. In the intermediate range of $f_p/f_{so} = 1.5$–3.5, the lock-on phenomenon prevails [12–18]. In this range, as the pulsation frequency f_p increases, the vortex shedding frequency f_s increases linearly with f_p. As f_p increases beyond this range, however, f_s displays a smooth transition toward the original value of f_{so}. Qualitatively similar trends are observed for all the blockage ratios.

Fig. 10 exhibits the regime diagrams in the plots of pulsating amplitude and frequency. The lock-on limits obtained in the present experiments are added to the previous results for in-line cylinder oscillations [17,18] and the flow pulsation for stationary circular cylinders [13,16]. The ordinate represents two different measures of the perturbation amplitude. For an in-line cylinder oscillation, the amplitude parameter is defined by the ratio of the peak to peak amplitude of cylinder displacement $2A$ and the cylinder diameter B. For flow pulsations, the normalized peak to peak velocity pulsation is given as $2A/\omega B$. As the Reynolds number increases, the lock-on regime broadens.

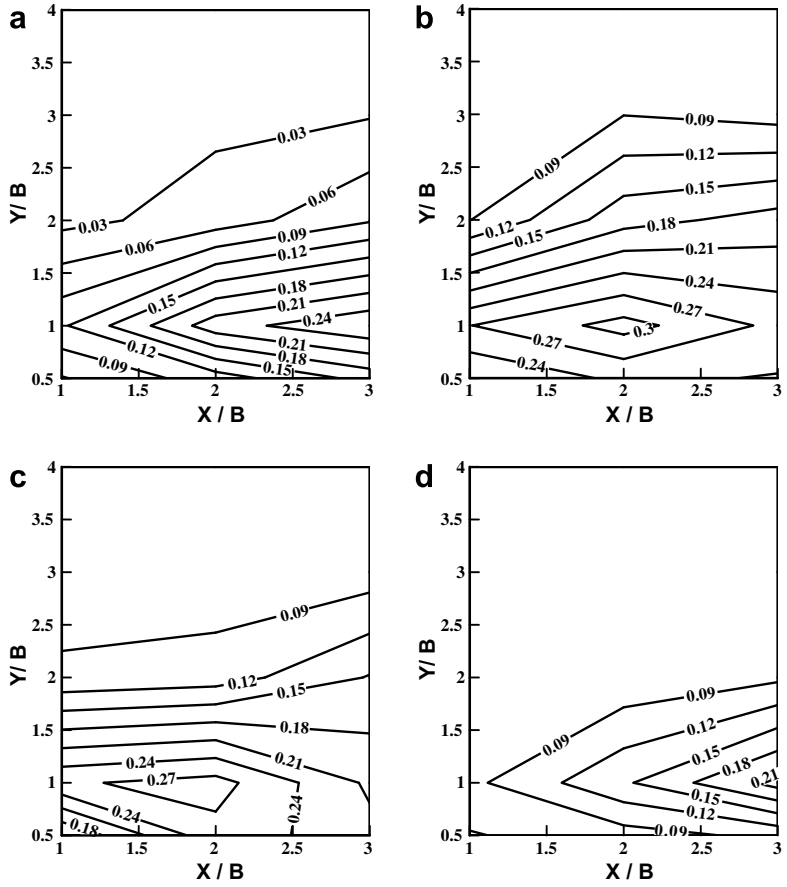

Fig. 8. Iso-lines of turbulence intensity in near-wake for various pulsating frequency at $Re = 540$, $\beta = 1/10$. (a) $f_p = 0$ Hz; (b) $f_p = 6$ Hz*; (c) $f_p = 10$ Hz*; (d) $f_p = 30$ Hz (* indicates lock-on).

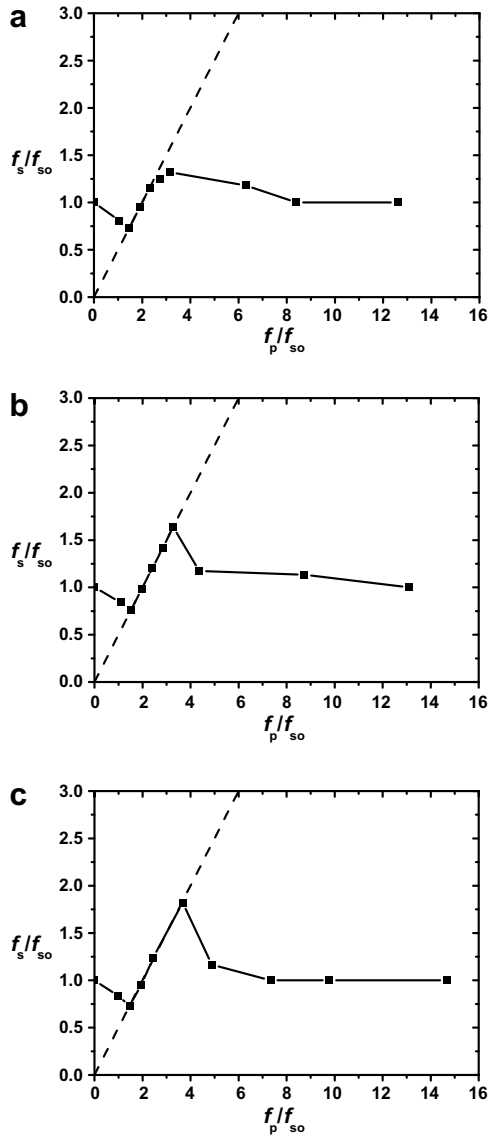

Fig. 9. The relationship between f_s and f_p at $Re = 540$; ---, $f_s/f_{so} = \frac{1}{2} f_p/f_{so}$. (a) $\beta = 1/6$, $f_{so} = 4.8$ Hz; (b) $\beta = 1/8$, $f_{so} = 4.6$ Hz; (c) $\beta = 1/10$, $f_{so} = 4.1$ Hz.

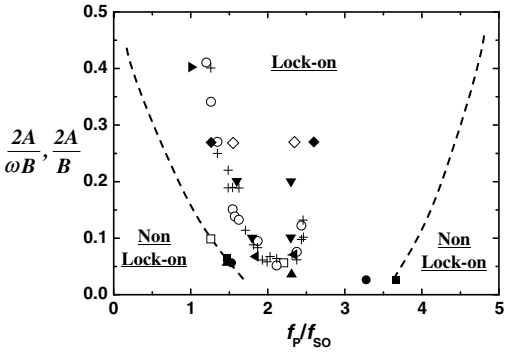

Fig. 10. Limits of the lock-on regime as a function of amplitude and frequency for in-line oscillations: ○, +, $Re = 190$ [18], ◇, $Re = 80$; ♦, $Re = 4000$ [17]; flow pulsations: ◄, $Re = 3000$; ►, $Re = 40\,000$ [13]; ▼, $Re = 200$ [16]; and the present study: □, $Re = 350$, $\beta = 1/10$; ■, $Re = 540$, $\beta = 1/10$; ●, $Re = 540$, $\beta = 1/8$; ▲, $Re = 540$, $\beta = 1/6$.

A similar trend was found in the previous results [13,17]. When the blockage ratio β increases from 1/10 to 1/6, the lock-on regime shrinks. It is attributed to the effect of confining walls [5].

The effect of Re on heat transfer enhancement factor E for various pulsating frequencies f_p at a fixed blockage ratio is displayed in Fig. 11. When the pulsating component of $A = 0.05$ is superimposed on the main incoming flow, heat transfer is substantially enhanced by interaction between the pulsation components and the vortices in the wake. It is noted that, when the pulsating frequency f_p is about twice the natural shedding frequency f_{so}, the heat transfer enhancement factor E shows a peak, which is indicative of lock-on. Outside this lock-on regime, the heat transfer enhancement is insignificant. This implies that the lock-on phenomenon is crucial in augmenting convective heat transfer from a heated cylinder [16,17]. As reported in the previous studies [13,15,18], when the lock-on happens, the vortices in the rear portions of the cylinder are more closely attached to the cylinder surface. Consequently, this results in heat transfer enhancement by flow pulsation. It is consistent with the finding in Fig. 8 about the changes in turbulence intensity level in the near-wake under the lock-on. As Re increases in Fig. 11b, the heat transfer enhancement factor increases [5,8].

Fig. 12 shows the influence of the blockage ratio on the heat transfer enhancement factor. As the blockage ratio

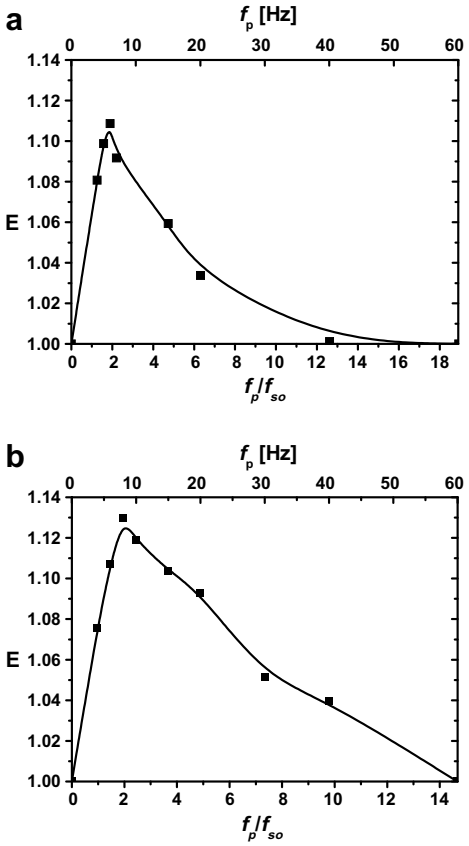

Fig. 11. The effect of Re on the heat transfer at $\beta = 1/10$. (a) $Re = 350$ ($f_{so} = 3.2$ Hz); (b) $Re = 540$ ($f_{so} = 4.1$ Hz).

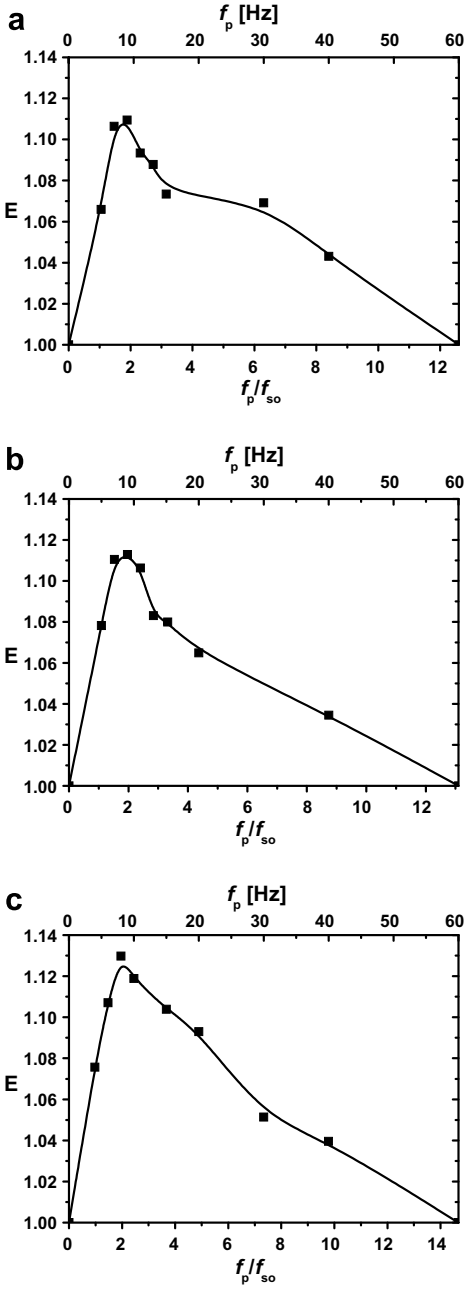

Fig. 12. The effect of β on the heat transfer at $Re = 540$. (a) $\beta = 1/6$ ($f_{so} = 4.8$ Hz); (b) $\beta = 1/8$ ($f_{so} = 4.6$ Hz); (c) $\beta = 1/10$ ($f_{so} = 4.1$ Hz).

decreases, the heat transfer enhancement factor E is more pronounced. As described in Fig. 10, this is due to the expansion of the lock-on regime as the blockage ratio decreases.

5. Conclusion

An experimental study was carried out to investigate convective heat transfer enhancement from a heated square cylinder in a pulsating channel flow. The effects of the pulsating frequency (0 Hz $< f_p <$ 60 Hz), the Reynolds number based on the mean velocity ($Re = 350$ and 540) and the blockage ratio ($\beta = 1/10$, 1/8 and 1/6) on heat transfer enhancement were examined. In addition, the influences of the Reynolds number and the blockage ratio in the lock-on regime diagrams were discussed.

In summary, the following conclusion is drawn from the present study:

(1) The occurrence of lock-on for a square cylinder was observed in the pulsating channel flow.
(2) As the Reynolds number increased and the blockage ratio decreased, the lock-on regime covered a wider parameter space.
(3) Heat transfer from the square cylinder increased within the lock-on regime. When the pulsating frequency was about twice the natural shedding frequency, i.e., under lock-on, the heat transfer enhancement factor E showed a peak.
(4) The heat transfer enhancement factor E was more pronounced with the increase of the Reynolds number and the decrease of the blockage ratio.

References

[1] M.M. Zdravkovich, Flow around Circular Cylinders, Oxford University Press, New York, 1997.
[2] C.H.K. Williamson, Vortex dynamics in the cylinder wake, Annu. Rev. Fluid Mech. 28 (1996) 477–539.
[3] A. Okajima, Strouhal numbers of rectangular cylinders, J. Fluid Mech. 123 (1982) 379–398.
[4] R.W. Davis, E.F. Moore, A numerical study of vortex shedding from rectangles, J. Fluid Mech. 116 (1982) 475–506.
[5] R.W. Davis, E.F. Moore, L.P. Purtell, A numerical–experimental study of confined flow around rectangular cylinders, Phys. Fluids 27 (1) (1984) 46–59.
[6] A. Mukhopadhyay, G. Biswas, T. Sundararajan, Numerical investigation of confined wakes behind a square cylinder in a channel, Int. J. Numer. Meth. Fluids 14 (1992) 1473–1484.
[7] H. Suzuki, Y. Inoue, T. Nishimura, K. Fukutani, K. Suzuki, Unsteady flow in a channel obstructed by a square rod (crisscross motion of vortex), Int. J. Heat Fluid Flow 14 (1) (1993) 2–9.
[8] M. Breuer, J. Bernsdorf, T. Zeiser, F. Durst, Accurate computations of the laminar flow past a square cylinder based on two different methods: Lattice-Boltzmann and finite-volume, Int. J. Heat Fluid Flow 21 (2000) 186–196.
[9] K.M. Kelkar, S.V. Patankar, Numerical prediction of vortex shedding behind a square cylinder, Int. J. Numer. Meth. Fluids 14 (1992) 327–341.
[10] K. Suzuki, H. Suzuki, Unsteady heat transfer in a channel obstructed by an immersed body, Annu. Rev. Heat Transfer 5 (1994) 174–206.
[11] S.Z. Shuja, B.S. Yilbas, M.O. Iqbal, Heat transfer characteristics of flow past a rectangular protruding body, Numer. Heat Transfer Part A 37 (2000) 307–321.
[12] H.J. Sung, K.S. Hwang, J.M. Hyun, Experimental study on mass transfer from a circular in pulsating flow, Int. J. Heat Mass Transfer 37 (15) (1994) 2203–2210.
[13] C. Barbi, D.P. Favier, C.A. Maresca, Vortex shedding and lock-on of a circular cylinder in oscillatory flow, J. Fluid Mech. 170 (1986) 527–544.
[14] O.M. Griffin, M.S. Hall, Review – Vortex shedding lock-on and flow control in bluff body wakes, J. Fluids Eng. 113 (1991) 526–537.

[15] A. Jarża, M. Podolski, Turbulence structure in the vortex formation region behind a circular cylinder in lock-on conditions, Eur. J. Mech. B Fluids 23 (2004) 535–550.
[16] M.R.H. Nobari, H. Naderan, A numerical study of flow past a cylinder with cross flow and inline oscillation, Comput. Fluids 35 (2006) 393–415.
[17] Y. Tanida, A. Okajima, Y. Watanabe, Stability of a circular cylinder oscillating in uniform flow or in a wake, J. Fluid Mech. 61 (1973) 769–784.
[18] O.M. Griffin, S.E. Ramberg, Vortex shedding from a cylinder vibrating in line with an incident uniform flow, J. Fluid Mech. 75 (1976) 257–271.
[19] D. Karanth, G.W. Rankin, K. Spidhar, A finite difference calculation of forced convective heat transfer from an oscillating cylinder, Int. J. Heat Mass Transfer 37 (11) (1994) 1619–1630.
[20] C.-H. Cheng, J.-L. Hong, W. Aung, Numerical prediction of lock-on effect on convective heat transfer from a transversely oscillating circular cylinder, Int. J. Heat Mass Transfer 40 (8) (1997) 1825–1834.
[21] W.-S. Fu, B.-H. Tong, Numerical investigation of heat transfer from a heated oscillating cylinder in a cross flow, Int. J. Heat Mass Transfer 45 (2002) 3033–3043.
[22] T.G. Beckwith, R.D. Marangoni, V. Lienhard, Mechanical Measurements, Addison Wesley Co Inc., New York, 1995.